

Low-Temperature Phases in Cs_2CdBr_4 and Cs_2HgBr_4

By D. ALTERMATT†

Institut für Kristallographie und Petrographie, ETH Zürich, ETH-Zentrum, CH-8092 Zürich, Switzerland

H. AREND

Laboratorium für Festkörperphysik, ETH Zürich, ETH-Hönggerberg, CH-8093 Zürich, Switzerland

AND V. GRAMLICH, A. NIGGLI AND W. PETTER

Institut für Kristallographie und Petrographie, ETH Zürich, ETH-Zentrum, CH-8092 Zürich, Switzerland

(Received 29 May 1983; accepted 19 March 1984)

Abstract

With respect to their phase transitions, Cs_2CdBr_4 and Cs_2HgBr_4 are the first known representatives of a new group having the $\beta\text{-K}_2\text{SO}_4$ -type structure. Upon cooling they show the following phase sequence. Phase I: $Pnma$, $Z = 4$. Cs, Cd/Hg and two Br are in special positions on the mirror plane. Second-order phase transition at T_{c1} . Phase II: satellites with $q \approx 0.15a^*$. First-order phase transition at T_{c2} . 'Lock-in' phase III: $P2_1/n$, $Z = 4$. Second-order phase transition at T_{c3} . Phase IV: $P\bar{1}$, $Z = 4$, no systematic absences in the X-ray patterns, doubling of the Br NQR frequencies. Cs_2HgBr_4 shows a further first-order transition at $T_{c4} = 85$ K with doubling of the Br NQR frequencies. Phase V: $P\bar{1}$, $Z = 8$, doubling of the b lattice constant. The values of the transition temperatures T_{c1} to T_{c3} are 252, 237 and 158 K for Cs_2CdBr_4 and 245, 232 and 167 K for Cs_2HgBr_4 . The phase transformations are explained by a rotation wave through the BX_4 tetrahedra. In $Pnma$ the wave has the appearance of a strong thermal motion. In the incommensurate phase the mode softens with a wavelength of about $7a$ and 'locks-in' with $k = 0$ (Γ point of the Brillouin zone) in $P2_1/n$. At 200 K the tetrahedra are turned around the a axis by 7° . In $P\bar{1}$ there is also a slight distortion of the structure.

Introduction

Reviews of known A_2BX_4 halides have been given by Arend, Mural, Plesko & Altermatt (1980), Altermatt (1983) and Arend, Mural, Altermatt & Chapuis (1984). Tetrahedrally coordinated A_2BX_4 halides of the $\beta\text{-K}_2\text{SO}_4$ type can be distinguished with respect to their phase transitions. There are polar (usually ferroelectric) low-temperature phases as well as centrosymmetric ones. In special cases, transitions

from tetrahedral to octahedral coordination (Rb_2MgCl_4 , Rb_2MnBr_4) have been reported from powder data analyses (Seifert & Fink, 1975; Seifert & Flohr, 1977; Goodyear, 1979). No phase transition could be found for Cs_2ZnBr_4 between room temperature and 5 K (Altermatt, Arend, Petter & Plesko, 1980; Plesko, Kind & Arend, 1980*b*). Four distinguishable phases for Cs_2CdBr_4 and five for Cs_2HgBr_4 have been identified between 20 K and room temperature by differential thermal analyses, nuclear quadrupole resonance measurements, Raman spectra, ultrasonic measurements and tests on piezoelectricity (Plesko, 1981; Plesko, Kind & Arend, 1980*a*; Plesko *et al.*, 1980*b*), *cf.* Fig. 1. The number of different NQR signals in this figure indicates the number of symmetrically different Br sites. All of the structures were characterized as centrosymmetric. Together with the results of X-ray film data based on Guinier-de Wolff powder photographs and precession photographs the phases and their transitions were determined as listed in the *Abstract*. The lattice constants listed in Table 1 were calculated from refinements of 25 diffractometer setting angles (with the exception of phase I, Cs_2HgBr_4 , where the results are based on powder photographs taken with a Jagodzinski camera). The lattice constants of phase V of Cs_2HgBr_4 could only be determined approximately because of experimental difficulties at the lower temperature limit of the diffractometer cryostat.

Experimental

The crystals were grown from a melt using the Bridgman technique. Purity of the melt was better than 99%. The experimental density of Cs_2CdBr_4 [Cs_2HgBr_4] is 4.15 (9) [4.61 (2)] g cm^{-3} , and the calculated density 4.09 (1) [4.62 (1)] g cm^{-3} . The samples for the X-ray investigations were cut from larger crystals by hand. Their shape was more or less cubic with edges of about 0.2 mm. Single-crystal data were collected on a Picker FACS-1 diffractometer with a

† Present address: Institute for Materials Research, McMaster University, Hamilton, Ontario, Canada L8S 4M1.

Table 1. *Lattice constants of Cs_2CdBr_4 and Cs_2HgBr_4*

	a (Å)	b (Å)	c (Å)	$\alpha = \beta = \gamma$ (°)	T (K)
Cs_2CdBr_4					
Phase I	10.228 (7)	7.931 (4)	13.966 (8)	90.0	295 (2)
Phase II			Incommensurate*		
Phase III	10.201 (10)	7.856 (7)	13.949 (12)	90.0 (2)	195 (1)
Phase IV	10.200 (27)	7.788 (16)	13.898 (31)	90.0 (3)	120 (3)
Cs_2HgBr_4					
Phase I	10.248 (1)	7.927 (1)	13.901 (1)	90.0	295 (2)
Phase II			Incommensurate*		
Phase III	10.162 (12)	7.813 (8)	13.796 (13)	90.0 (2)	200 (1)
Phase IV	10.148 (12)	7.754 (9)	13.837 (17)	90.0 (2)	120 (3)
Phase V	10.1 (2)	15.4 (2)	13.8 (2)	90 (3)	80 (3)

* No significant differences between the lattice constants of phase I and those of the basic structure of phase II were observed.

closed cryostat, cooled by liquid nitrogen (see Coppens, Ross, Blessing, Cooper, Larson, Leipolt, Rees & Leonhard, 1974; Lenhart, 1975). The temperature stability was ± 0.1 K at room temperature, ± 0.2 K at 230 K, ± 1 K at 160 K and ± 3 K at 120 K. The measurements were made with Mo $K\alpha$ radiation and a perpendicularly mounted graphite monochromator. Intensities were measured from 0 to 50 [0 to 40] $^\circ$ (2θ) using a continuous scan technique.

An experimental correction for absorption was made using the technique of Flack (1977). Reflexions were tagged unobserved if $I < 3\sigma(I)$ for the room-temperature structures, and if $I < 6\sigma(I)$ for the struc-

tures measured in the closed cryostat. In the least-squares refinements the following weights were used: $w = 1/\sigma(I)$ for the room-temperature structures and $w = 1$ for all others. Ionic scattering factors were taken from Cromer & Mann (1968).

Results and discussion

All computational work was performed on CDC computers at the ETH-Zürich computing center with the XRAY system of crystallographic programs (Stewart, Kruger, Ammon, Dickinson & Hall, 1972). The final parameters of Cs_2HgBr_4 and Cs_2CdBr_4 have been deposited.†

The room-temperature phase (phase I) of Cs_2CdBr_4 has already been reported (Altermatt, Niggli, Petter & Arend, 1979). This phase, as well as phase I of Cs_2HgBr_4 , is isostructural with $\beta\text{-K}_2\text{SO}_4$, i.e. $Pnma$, $c:b \approx \sqrt{3}:1$, with pseudohexagonally arranged, isolated tetrahedra (cf. Figs. 2a, 2b). The anisotropic shape of the Br atoms can be interpreted as thermal motion since static disorder is excluded by the unique NQR signals of Fig. 1.

For the incommensurate phase II a unique structural model could not be found. Very few and very weak satellites of first order only could be observed at $q \approx 0.15a^*$. No satellites appear at the $h00$ reflexions nor around the space-group-extinct reflexions $0kl$, $k+l=2n+1$ (n glide), whereas some satellites are observable around $hk0$, $h=2n+1$ (a glide). A special feature of the $hk0$ pattern is that satellites are observed for $h=0$ and k even.

The basic structure of phase II is not significantly different from the structure of phase I. It has been shown by Plesko (1981) that the soft mode leading to the incommensurate phase belongs to the Σ_2 representation for $q \neq 0$ and to Γ_4^+ at the Γ point of the Brillouin zone (see also Plesko *et al.*, 1980b). Since the two representations are compatible (Plesko, 1981), the superspace-group assignment of Janssen & Janner (1980) for the Σ_2 mode, P_{155}^{Pnma} , can be adopted here which is equivalent to the space group $62c.9.2$ of the tables of de Wolff, Janssen & Janner (1981) (P. M. de Wolff, 1983, private communication). However, there are some satellites violating the extinction rules for $(\frac{a}{2})$, $hk0m$, $h+m=2n$ and for $(\frac{m}{2})$, $h0lm$, $m=2n$: first-order satellites around 020 , 040 and 060 are observable. They cannot be neglected since they are among the most intense satellite reflexions. In the $h0l$ plane several first-order satellites are observed which conflict with $(\frac{m}{2})$. They occur around $30l$, $l=1, \dots, 4$; 403 ; 405 ; 503 ; 504 ; 507 and 601 . Therefore, the

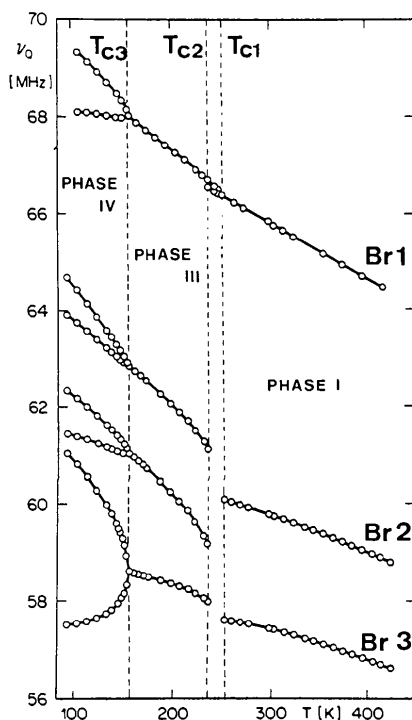
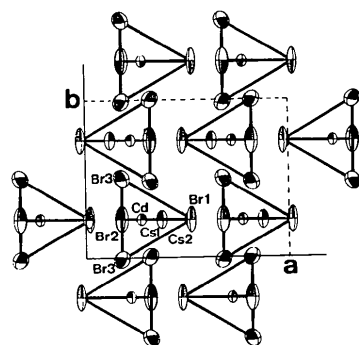
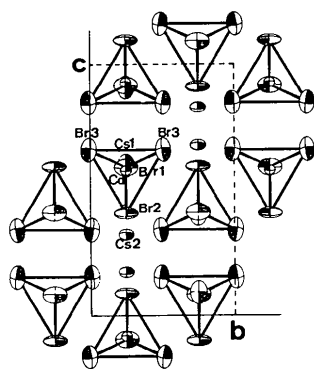


Fig. 1. Temperature dependence of the ^{81}Br NQR frequencies for Cs_2CdBr_4 and assignments of the signals to the Br sites according to Plesko *et al.* (1980a).

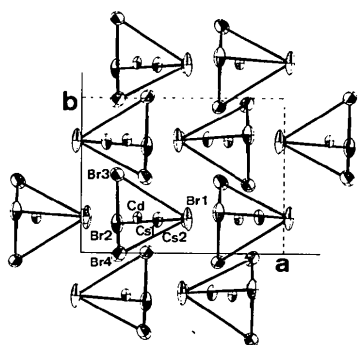
† Lists of structural parameters and structure factors of phases I and III of Cs_2HgBr_4 and Cs_2CdBr_4 and of phase IV of Cs_2CdBr_4 have been deposited with the British Library Lending Division as Supplementary Publication No. SUP 39319 (89pp.). Copies may be obtained through The Executive Secretary, International Union of Crystallography, 5 Abbey Square, Chester CH1 2HU, England.



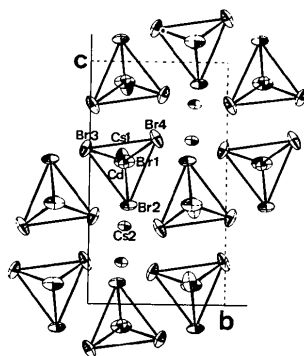
(a)



(b)



(c)



(d)

Fig. 2. Projections of the phases I and III of Cs_2CdBr_4 : (a), (b) Room temperature phase I. (c), (d) 'Lock-in' phase III.

Table 2. Atomic parameters for Cs_2CdBr_4 in $P2_1/n$

The equivalent isotropic temperature factors B_{eq} have been calculated by $B_{\text{eq}} = \frac{8}{3} \pi^2 \sum_i \sum_j U_{ij} a_i^* a_j^* \cdot a_i \cdot a_j$.

	x	y	z	$B_{\text{eq}}(\text{\AA}^2)$
Cs(1)	0.1224 (1)	0.2596 (2)	0.0997 (1)	4.9 (1)
Cs(2)	-0.01579 (9)	0.2595 (1)	0.67559 (7)	2.6 (1)
Cd	0.2226 (1)	0.2472 (1)	0.42431 (7)	2.0 (1)
Br(1)	-0.0264 (2)	0.2532 (3)	0.4140 (1)	4.8 (2)
Br(2)	0.3228 (2)	0.2875 (3)	0.5917 (1)	3.6 (2)
Br(3)	0.3237 (2)	-0.0312 (2)	0.3623 (2)	4.2 (2)
Br(4)	0.3131 (2)	0.4844 (2)	0.3176 (2)	4.8 (2)

Measured reflections	4389
Unique reflections	1639
Unobserved reflections	462
R value (without unobserveds)	0.036
Temperature	195 ± 1 K

maximum symmetry should be lowered, e.g. to $P_{11}^{21/n}$ (or 14b.5.1) according to the tables of de Wolff *et al.* (1981).

A model with all four tetrahedra in the unit cell of the basic structure being turned in phase by a rotation wave r_x has been proposed by Plesko (1981). The extinction rules mentioned above can be confirmed by inspection of Fig. 2 if such a rotation wave is considered. This model is highly persuasive because it agrees with the refined 'lock-in' phase (see below) and the NQR measurements. The rotation wave explains further the absence of satellites at the $h00$ reflexions, whereas a transverse wave would require the absence of satellites in a whole reciprocal-lattice plane. Finally the model explains the absence of satellites in the $hk0$ plane around the non-extinct reflexions $h = 2n$, $h \neq 0$. Nevertheless, the observed satellites for $0k0$, $k = 2n$ are in conflict with the model, so that no satisfactory explanation of this $hk0$ pattern is presently available.

The intensity distribution of phase III shows nearly orthorhombic symmetry. The extinction for the a -glide plane is no longer fulfilled. Since the space group of phase III was found to be centrosymmetric (Plesko, 1981), the monoclinic space group $P2_1/n11$ was chosen according to the observed n -glide extinctions. The approximate orthorhombic symmetry of the data set was explained by a probability $p \approx 0.5$ of the two possible domain orientations of the monoclinic phase with respect to the orthorhombic one (*cf.* Dunitz, 1979, p. 57). The starting model for the monoclinic structure was the $r_x(111)$ model of Plesko (1981) for the limiting case $q = 0$. The decomposition of the observed intensities into the monoclinic ones was managed by a local program compatible with the XRAY system. After each least-squares cycle the division of the orthorhombic $F_{\text{obs}}(hkl)$ into the monoclinic $F'_{\text{obs}}(hkl)$ and $F'_{\text{obs}}(hk\bar{l})$ was updated with the conditions

$$\frac{1}{2} [|F'_{\text{obs}}(hkl)|^2 + |F'_{\text{obs}}(hk\bar{l})|^2] = |F_{\text{obs}}(hkl)|^2$$

and

$$|F'_{\text{obs}}(hkl)|^2 : |F'_{\text{obs}}(hk\bar{l})|^2 = |F'_{\text{calc}}(hkl)|^2 : |F'_{\text{calc}}(hk\bar{l})|^2.$$

The procedure converged at rather small deviations from the orthorhombic structure (Fig. 2*c, d*) which justified the use of the orthorhombic standard deviations in the monoclinic refinement. All tetrahedra in phase III are simultaneously rotated by 7–8° around the *a* axis and are slightly displaced in the *b* direction. There is no rotation around the *c* axis (which would be allowed by symmetry). Table 2 gives the parameters for Cs₂CdBr₄ in *P*2₁/*n*.

In the triclinic phase IV the structure undergoes an additional slight distortion. The conditions for the *n* glide are no longer fulfilled; therefore, possible space groups *P* $\bar{1}$ or *P*2₁ can be considered for that phase. The diffraction patterns of the two Cd and Hg compounds are again very similar. No persuasive starting model was feasible. Nevertheless, several starting models for Cs₂CdBr₄ in *P* $\bar{1}$ yielded the same result whereas refinements in *P*2₁ were less satisfactory. Experimental difficulties with the closed cryostat prohibited the measurement of a complete data set of phase IV for the Hg compound.

No unusual distances or angles were observed in any phase and the small changes in the internal structure of the BX₄ tetrahedra at the phase transitions are probably not significant. However, the rotations of the BX₄ tetrahedra in the lower phases lead to large changes in the environment of the Cs atoms. The main driving force for the phase transformations is the tension between Cs–Br attractions and Br–Br repulsions. The cavities around the two Cs positions have different sizes. The large cavity around Cs(1) is defined by 11 Br atoms, the smaller around Cs(2) by 9 Br atoms at distances in the range between 3.6 and 4.7 Å. The calculated valence (Brown, 1981)* around Cs(1) is much smaller than expected. This is characteristic of an atom in a cavity that is too large. Such a situation is unstable and can lead to a displacive phase transition in which the environment changes in such a way as to increase the bond-valence sum (Brown, 1978). This effect is observed in these compounds around Cs(1) but not around Cs(2) for which

the bonding is already satisfactory. Thus for Cs₂CdBr₄ the valence sum around Cs(1) is 0.53 and around Cs(2) 1.02 in the high-temperature *Pnma* phase. On cooling to the *P*2₁/*n* phase the Cs(1) valence increases to 0.63 but the Cs(2) valence remains at 1.01. Further cooling to the *P* $\bar{1}$ phase increases the valence of Cs(1)/Cs(11) further to 0.70 but that of Cs(2)/Cs(12) increases only slightly to 1.06.

Helpful comments of Professors P. M. de Wolff and I. D. Brown are gratefully acknowledged.

References

- ALTERMATT, D. (1983). *Kristallographische Untersuchungen der Phasenfolgen von Cs₂CdBr₄ und Cs₂HgBr₄*. Diss. No. 7241. Swiss Federal Institute of Technology, Zürich, Switzerland.
- ALTERMATT, D., AREND, H., PETTER, W. & PLESKO, S. (1980). *Joint Italo-Swiss Meeting on Crystallography*, Trento/1. Abstracts, p. 3.
- ALTERMATT, D., NIGGLI, A., PETTER, W. & AREND, H. (1979). *Mater. Res. Bull.* **14**, 1391–1396.
- AREND, H., MURALT, P., ALTERMATT, D. & CHAPUIS, G. (1984). *Ferroelectrics*. In preparation.
- AREND, H., MURALT, P., PLESKO, S. & ALTERMATT, D. (1980). *Ferroelectrics*, **24**, 297–303.
- BROWN, I. D. (1978). *Chem. Soc. Rev.* **7**, 359–376.
- BROWN, I. D. (1981). *Structure and Bonding in Crystals*. Vol. II, pp. 1–30. New York: Academic Press.
- COPPENS, P., ROSS, F. K., BLESSING, R. H., COOPER, W. T., LARSON, F. K., LEIPOLT, J. G., REES, B. & LEONHARD, L. (1974). *J. Appl. Cryst.* **7**, 315–319.
- CROMER, D. T. & MANN, J. B. (1968). *Acta Cryst.* **A24**, 321–324.
- DUNITZ, J. D. (1979). *X-ray Analysis and the Structures of Organic Molecules*. Ithaca and London: Cornell Univ. Press.
- FLACK, H. D. (1977). *Acta Cryst.* **A33**, 890–898.
- GOODYEAR, J. (1979). *Acta Cryst.* **B35**, 456–457.
- JANSSEN, T. & JANNER, A. (1980). *Ferroelectrics*, **24**, 11–17.
- LENHERT, P. G. (1975). *J. Appl. Cryst.* **8**, 568–570.
- PLESKO, S. (1981). *Neue Folge von kommensurablen und inkommensurablen Phasen in Kristallen vom β-K₂SO₄ Typ*. Diss. No. 6929. Swiss Federal Institute of Technology, Zürich, Switzerland.
- PLESKO, S., KIND, R. & AREND, H. (1980*a*). *Ferroelectrics*, **26**, 703–706.
- PLESKO, S., KIND, R. & AREND, H. (1980*b*). *Phys. Status Solidi A*, **61**, 87–94.
- SEIFERT, H. J. & FINK, H. (1975). *Rev. Chim. Minér.* **12**, 466–475.
- SEIFERT, H. J. & FLOHR, G. (1977). *Z. Anorg. Allg. Chem.* **436**, 244–252.
- STEWART, J. M., KRUGER, G. J., AMMON, H. L., DICKINSON, C. W. & HALL, S. R. (1972). The XRAY system. Computer Science Center, Univ. Maryland, College Park, Maryland. Revised by D. SCHWARZENBACH (1976), Univ. Lausanne, Switzerland.
- WOLFF, P. M. DE, JANSSEN, T. & JANNER, A. (1981). *Acta Cryst.* **A37**, 625–636.

* The parameters in the valence calculations have been chosen so that the sum around Cs(2) in *Pnma* becomes approximately 1; $s = \exp[(2.96 - R)/0.35]$.